Miniaturized Electrostatic Size Classifier (mESC): Development and Validation of Nanometer Aerosol Classification

Papol Sardyoung[1] and Panich Intra[2*]
[1]Department of Industrial Electrical Technology, Faculty of Industrial Technology, Thepsatri Rajabhat University, Mueang Lopburi, Lopburi, Thailand
[2]Research Unit of Applied Electric Field in Engineering College of Integrated Science and Technology, Rajamangala University of Technology Lanna, Chiang Mai, Thailand
E-mail: papol.s@lawasri.tru.ac.th, panich.intra@rmutl.ac.th[*]

Received: January 26, 2026 / Revised: April 10, 2026 / Accepted: April 22, 2026

***Abstract*— This study focuses on developing and testing the preliminary performance of a miniaturized electrostatic classifier for nanometer-sized aerosol particles. Designed with a parallel-plate configuration, the prototype classifies aerosols up to 300 nm in diameter. We first developed a mathematical model to accurately predict particle trajectories across sizes within the classifier. The physical prototype was then evaluated for its size-classification capabilities. Experimental findings showed strong agreement with theoretical predictions, confirming the model's effectiveness in designing such electrostatic classifiers. Furthermore, the prototype demonstrates promising potential for accurately classifying nanometer-sized aerosol particles.**

***Index Terms*— Aerosol, Nanoparticle, Miniature, Electrostatic, Size Classifier**

I. Introduction

Nanoparticles are particles characterized by diameters in the nanometer size range [1], [2], resulting from various chemical, physical, or biological processes. These particles are widely recognized for their technological importance across numerous disciplines. They are integral to fields such as materials synthesis, biotechnology, semiconductor manufacturing, pharmaceutical development, nanocomposites and ceramics, emission control, health effects studies, measurement and instrumentation, and fundamental investigations into transfer processes.

As particle size is a key physical characteristic that profoundly influences their behavior and dynamics, accurate measurement and classification are crucial. These activities are essential for better understanding particle transport, controlling contamination, and generating monodisperse particle samples needed for research.

Among the diverse techniques established for nanoscale aerosol particles, the electrical mobility analyzer has become the gold-standard instrument for both classifying and generating monodisperse particles. Electrical mobility measurements have a long history, dating back to the early twentieth century. This method of determination was initially applied to measure gaseous ions [3] and atmospheric ions [4]-[6]. Subsequently, Rohmann [7] was instrumental in utilizing this technique to quantify airborne particles in the atmosphere.

A typical electrical mobility analyzer (often referred to as a Differential Mobility Analyzer, or DMA) is generally constructed with two concentric electrodes between which a voltage is applied. An aerosol containing charged particles is introduced near one of the electrodes. Crucially, a particle-free sheath airflow separates the aerosol from the opposing electrode. The electric field established across the gap causes charged particles to migrate toward the opposing electrode. Since a particle's migration speed is directly proportional to its electrical mobility (which correlates with its size), particles exit the analyzer at different axial positions according to their size.

The electrical mobility analyzer has been the subject of continuous investigation and innovation, with recent developments comprehensively summarized by Flagan [8] and Intra and Tippayawong [9].

A significant portion of earlier research [10]-[16] has focused on refining performance through single-size channel identification, enhancing measurement capabilities, and expanding the instrument's operational size range.

More recently, the scientific community has seen a growing trend toward miniaturization of these analytical instruments. This shift aims to create instruments that are more portable, less expensive, and easier to deploy in various field settings while

maintaining high analytical accuracy. Such miniaturized DMAs (mDMAs) address the limitations of conventional benchtop instruments, which are often bulky and power-intensive.

This study contributes to the field by developing a miniature electrostatic classifier that accurately classifies nanometer-sized aerosol particles, operating on principles similar to those of its predecessors. However, the present analyzer distinguishes itself from existing instruments through the following key innovations:

1) Compact Design and Portability: The instrument was specifically engineered to be a small, cost-effective, and highly portable device. To minimize particle diffusion, we intentionally adopted a short classifier length. Its optimized dimensions and light weight improve handling and field mobility.

2) Controlled Operating Voltage: The applied voltage was maintained at a low level, significantly below the corona initiation voltage, to prevent any inadvertent or undesirable charging of particles within the classifier volume.

This research began by establishing a mathematical model to accurately predict particle trajectories inside the classifier for different particle sizes. This model then served as the foundation for designing the complete aerosol size spectrometer system. The final step involved experimentally testing the physical classifier prototype to comprehensively evaluate its aerosol size-classification performance.

Research Objectives: The primary goal of this study is to develop and validate a high-performance miniature electrostatic classifier. The specific objectives are as follows:

A. Design and Instrumentation

1) Mechanical Design: Develop a compact parallel-plate (or radial) classifier geometry optimized for a target size range of X-Y nm.

2) Flow Dynamics: Engineer the internal manifold to maintain stable, laminar sheath-to-aerosol flow ratios at Z flow rates, ensuring a distinct separation between particle trajectories.

3) Voltage Regulation: Implement a control system to maintain operating voltages significantly below the corona discharge threshold to prevent unintended particle charging and electrical noise.

B. Mathematical Modeling and Validation

1) Trajectory Prediction: Derive a robust mathematical model based on the balance of electrical drag and convective forces to predict the exit particle diameter (nm) as a function of the applied voltage (kV) and flow rate liters per minute (lpm).

2) Model Validation: Validate the theoretical transfer function against numerical simulations to account for non-ideal effects such as flow distortions at the inlet/outlet.

C. Performance Evaluation

1) Classification Accuracy: Determine the Geometric Standard Deviation (GSD) of the output aerosol to assess the instrument's ability to generate truly monodisperse samples.

2) System Reliability: Conduct longitudinal testing to evaluate the repeatability of measurements across multiple duty cycles and environmental conditions.

3) Loss Analysis: Quantify internal particle losses caused by diffusion and electrostatic attraction to non-target surfaces, particularly for particles under 20 nm.

D. Comparative Benchmarking

1) Standard Correlation: Perform side-by-side experimental runs with a commercial-grade DMA/SMPS (Scanning Mobility Particle Sizer) to correlate sizing accuracy and concentration measurements.

2) Efficiency Analysis: Compare the power consumption, weight, and response time of the prototype against the standard benchtop system to justify its use in portable applications.

Table I is a comparison between the prototype Miniaturized Electrostatic Size Classifier (mESC) evaluated in the study and conventional benchtop Differential Mobility Analyzers (DMAs):

TABLE 1
TECHNICAL SPECIFICATIONS COMPARISON: MESC PROTOTYPE VS. CONVENTIONAL BENCHTOP DMAS

Feature	mESC Prototype	Conventional Benchtop DMA
Device Type	Miniature Electrostatic Size Classifier (mESC)	Differential Mobility Analyzer (DMAs) / Standard Benchtop System
Geometry	**Parallel-plate configuration** consisting of two metal plates separated by a 2.5 mm gap	Generally constructed with **two concentric electrodes**
Size Range	Designed to classify nanometer-sized aerosol **up to 300 nm** in diameter	Measures broad nanoscale aerosol particles (specific numerical range is not detailed in the sources)
Flow	Engineered for a **1.0 L/min sheath flow rate**, and tested using a 0.6 L/min aerosol flow with total flow rates ranging up to 2.4 L/min	Utilizes a particle-free sheath air flow to separate the aerosol from the opposing electrode

TABLE 1
TECHNICAL SPECIFICATIONS COMPARISON: MESC PROTOTYPE VS. CONVENTIONAL BENCHTOP DMAS (CONT.)

Feature	mESC Prototype	Conventional Benchtop DMA
Voltage	Tested at low-level applied DC voltages from **0.5 kV to 2.5 kV** to prevent inadvertent particle charging, though the physical gap allows for a theoretical breakdown limit of roughly 7.5 kV	Operates by applying a voltage between the two concentric electrodes to establish an electric field (specific operational voltages are not listed)
Footprint	Highly compact and portable, measuring exactly **120 mm (L) × 80 mm (W) × 40 mm (H)**	Larger, standard benchtop systems that are generally less portable, heavier, and more expensive to deploy in field settings

II. SCHEMATIC DESCRIPTION OF THE MINIATURE ELECTROSTATIC SIZE CLASSIFIER

The schematic diagram of the prototype miniature electrostatic classifier is illustrated in Fig. 1, Classifier Core and Structure. The classifier utilizes a parallel-plate configuration, consisting of two metal plates separated by a 2.5 mm gap. This gap defines the height of the size classification zone. To minimize electrostatic particle losses during aerosol transport, the metal plates were designed with separate channels for polydisperse and classified aerosol flows. For safety, these two metal electrode plates are housed in a Teflon enclosure and electrically insulated.

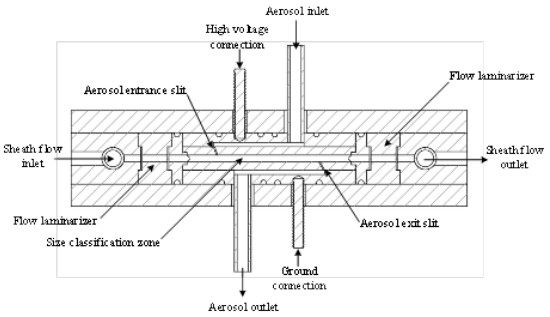

Fig. 1. Schematic diagram of the studied miniature electrostatic classifier

A. Aerosol and Sheath Flow Configuration

1) Aerosol Inlet: The polydisperse aerosol flow is introduced at the top inlet of the classifier. It subsequently passes through a triangular-shaped flow channel before entering the classification zone via the Aerosol entrance slit.

2) Electrodes and Field: A positive high DC voltage is applied to the top electrode plate (high-voltage connection), while the bottom electrode plate is electrically grounded (Ground connection). This setup establishes a uniform electric field within the particle-size classification zone.

3) Sheath Flow: Sheath air enters the classifier through the left inlet, passing through a screen-type flow linearizer to ensure a smooth, stable flow profile before reaching the classification zone. The excess flow then exits the classifier through the right-side outlet (Sheath flow outlet).

4) Classified Aerosol Outlet: The channel for the classified aerosol (Aerosol outlet) in the bottom metal plate is designed symmetrically to the inlet channel.

B. Design Parameters and Performance Goal

The geometry of the core components was precisely engineered:

1) Slits: The slits for aerosol entrance and exit are 2 mm long and 0.5 mm wide. Using a shorter slit length relative to the classification zone width helps keep aerosol flow away from the classifier's side walls, mitigating particle wall loss. The center-to-center distance between the entrance and exit slots is 40 mm.

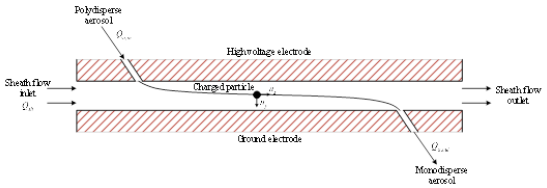

Fig. 2. Schematic diagram of particle trajectory in studied miniature electrostatic classifier

Performance: The prototype M-EC was engineered to classify particles up to 300 nm in diameter at a sheath flow rate of 1.0 liters per minute (lpm).

Footprint: The prototype's overall dimensions are remarkably compact, measuring 120 mm in length, 80 mm in width, and 40 mm in height, underscoring its miniature, portable design.

Fig. 2 illustrates the fundamental principle of particle classification by depicting a schematic of a charged particle's trajectory within the miniature electrostatic classifier. Particle Motion Dynamics: The movement of a particle inside the classification zone is governed by two primary forces, resulting in two distinct velocity components:

a) Axial Motion (u_z): The particle's motion along the length of the classifier (z-axis) is dictated by the fluid velocity profile of the combined sheath and aerosol flows. Since the flow is typically laminar, the particle is carried axially along the flow streamlines.

b) Radial Motion (u_r): The particle's lateral movement (r-axis) is primarily driven by the electric force. For nanometer-sized aerosols, the electric force is significantly stronger than other lateral forces, such as gravity or diffusion, making it the dominant factor in radial transport. Classification Mechanism, when a charged particle enters the size classification zone, the

applied electric field causes it to acquire an electrical mobility. This mobility, inversely proportional to the particle's size, determines how quickly the particle migrates radially toward the grounded electrode.

As shown in the diagram, polydisperse aerosol (Q_a,in) is introduced, and depending on a particle's electrical mobility (and thus its size), it follows a specific curved path. Only particles with a narrow range of mobilities will successfully exit through the Aerosol outlet (Q_a,out), resulting in a monodisperse aerosol sample. Particles outside this range will either deposit on the collection electrode or be carried out with the sheath-flow outlet.

It is assumed that: The flow and electric fields are axisymmetric and steady, the flow in the classifier is laminar, fully developed, and incompressible ($\nabla \cdot u = 0$), the space charge effect is negligible ($\nabla \cdot E = 0$), and the gravitational and Brownian diffusion effects are negligible. The total volumetric flow rate,Q_t, through the classifier column is

$$Q_t = Q_{sh} + Q_a \tag{1}$$

where Q_{sh} is the particle-free sheath air flow rate and Q_a is the aerosol flow rate. For the particular case of annular geometries where the charged aerosol sample enters the classifier on an axial flow, and the charged particles migrate along the radial direction of the electric field, the motion of the charged particles within the classification zone can be described by the system of differential equations as [17].

$$\frac{dy}{dt} = u_y + Z_p E_y \tag{2}$$

$$\frac{dz}{dt} = u_z + Z_p E_z \tag{3}$$

Where y and z are the radial and axial dimensions of the classifier, u_y and u_z are the radial and axial components of the air flow velocity. Similarly, E_y and E_z are the radial and axial components of the electric field and Z_p is the electrical mobility of particles. When a uniform electric field is established between the two electrodes of the classifier, the electric field components are given by the following relations

$$E_y = \frac{V}{h} \quad \text{and} \quad E_z \approx 0 \tag{4}$$

where V is the applied electrode voltage and h is the height of the classifier. Assuming uy = 0 and uz = uz(y). Substituting into Equations (2) and (3) gives the following differential equations describing the trajectory of an aerosol particle in a viscous flow [17],

$$\frac{dy}{dt} = \frac{Z_p V}{h} \tag{5}$$

$$\frac{dz}{dt} = u_z(y) \tag{6}$$

where:

$$u_z(y) = \frac{h^2}{2\mu}\left(-\frac{dp}{dz}\right)\left(\frac{1}{4} - \frac{y^2}{h^2}\right) \tag{7}$$

dp/dz represents the constant pressure gradient, defined by equations

$$\frac{dp}{dz} = -\frac{\rho \bar{U}^2 f}{2D_h} \tag{8}$$

Where:

$$D_h = 2h, \tag{9}$$

$$f = \frac{96}{Re} \tag{10}$$

$$Re = \frac{\bar{U}\rho D_h}{\mu}, \tag{11}$$

D_h Is the hydraulic diameter for an annular flow area f is the friction factor, $\bar{U}$ is the mean axial flow velocity, ρ is the gas density and Re is the Reynolds number in the annular flow. Using Equations (5) and (6), the trajectory of the charged particle in a viscous flow is given by

$$\frac{dy}{dz} = \frac{\frac{dy}{dt}}{\frac{dz}{dt}} = \frac{Z_p V}{u_z(r)h} \tag{12}$$

Integrating Equation (12), the migration paths of the charged particles can be determined. Their landing location downstream of the aerosol inlet is given in terms of their electrical mobility, the flow velocity profile, and the electric field strength:

$$\frac{h^2}{2\mu}\left(-\frac{dp}{dz}\right)\int_0^y \left(\frac{1}{4} - \frac{y^2}{h^2}\right) dy = \frac{VZ_p}{h}\int_0^z dz \tag{13}$$

The particle entering the classifier at a radial position of has a trajectory taking it to an axial position of z, which can be obtained as

$$z = -\frac{y}{VZ_p}\left(-\frac{h^2}{2\mu}\frac{dp}{dz}\left(\frac{y}{4} - \frac{y^3}{3h^2}\right)\right) \tag{14}$$

Which rearranges in terms of the critical electrical mobility of y a particle that is collected on the electrode at a distance z downstream of the aerosol inlet can be calculated as

$$Z_p = -\frac{y}{Vz}\left(-\frac{h^2}{2\mu}\frac{dp}{dz}\left(\frac{y}{4} - \frac{y^3}{3h^2}\right)\right) \tag{15}$$

C. Experimental Setup for Performance Evaluation

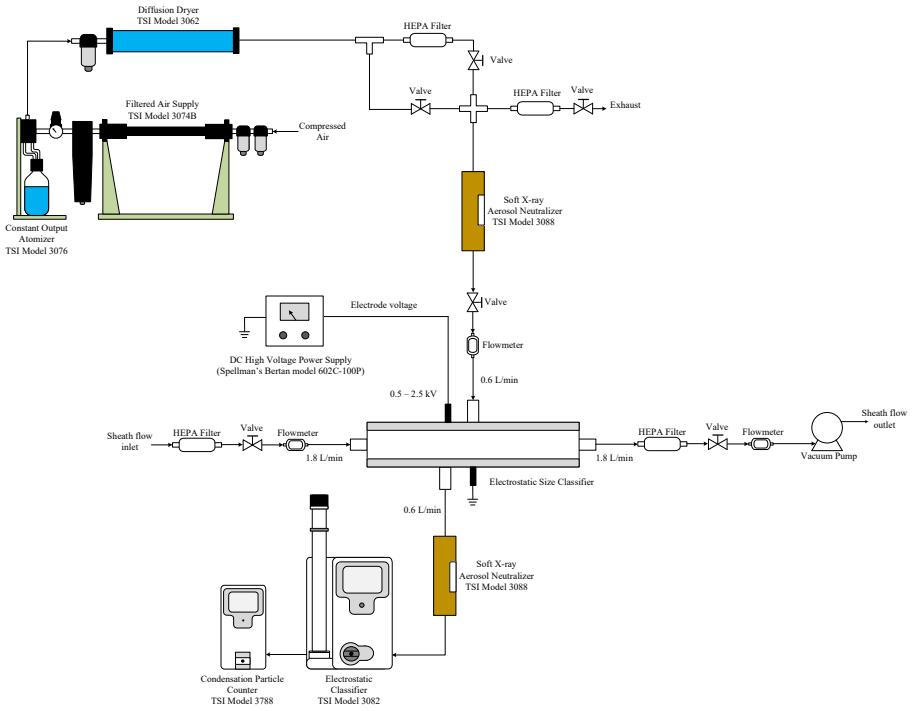

Fig. 3. Experimental setup for the performance evaluation of the miniature electrostatic classifier

Fig. 3 presents the comprehensive experimental setup used to evaluate the performance of the miniature electrostatic size classifier. System Components and Aerosol Generation The integrated system comprises several standard components, including an aerosol atomizer, a filtered air supply, an aerosol neutralizer, concentration adjustment valves, a HEPA filter, a diffusion dryer, flowmeters, a vacuum pump, a DC high-voltage power supply, the electrostatic classifier under investigation, and an Ultrafine Condensation Particle Counter (UCPC). Sodium Chloride (NaCl) polydisperse particles were generated by atomizing a 0.1% (w/w in water) NaCl solution using an Aerosol Atomizer (TSI Model 3076) paired with a Filtered Air Supply (TSI Model 3074B). The resulting wet NaCl particles were then passed through a Diffusion Dryer (TSI Model 3062) to reduce the relative humidity to below approximately 30% RH. Aerosol Conditioning and Characterization.

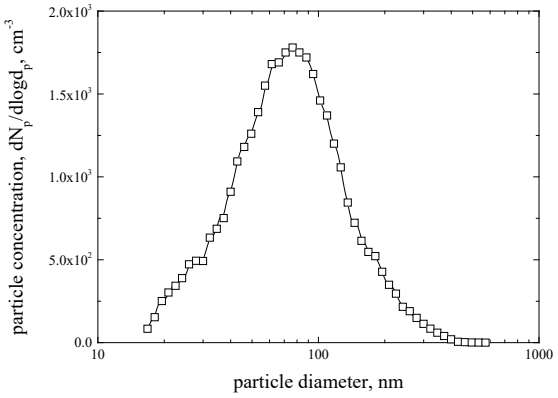

Fig. 4. Particle concentration and size distribution of sodium chloride particles generated from an atomizer

The generated NaCl particles inherently carry some electric charge. Failure to neutralize these charges could lead to significant particle losses due to electrostatic deposition on the inner walls of the tubing and other surfaces within the system. Therefore, a Soft X-ray Aerosol Neutralizer (TSI Model 3088) was employed to bring the particles to their Boltzmann charge equilibrium state. Particle number concentration could be precisely regulated by adjusting the concentration adjustment valves in combination with a HEPA capsule filter. Fig. 4 presents the particle concentration and size distribution of the polydisperse sodium chloride (NaCl) aerosol generated by the atomizer and conditioned by the system.

Analysis of the generated aerosol confirms that the particles follow a log-normal distribution. Specifically, the polydisperse NaCl aerosol utilized for the performance evaluation exhibited a mean particle diameter of 98.8 nm, a total number concentration of 1.74 x 10^3 particles/cm^3, and a geometric standard deviation (sigma_g) of 2.0. This distribution served as the input challenge aerosol for the miniature electrostatic classifier. Classifier Operation and Measurement

The prepared polydisperse NaCl particles were introduced into the classifier under study for size classification based on their electrical mobility. The classifier was operated at a target aerosol flow rate (Q_a,in) of 0.6 L/min and a sheath flow rate (Q_sh) of 1.8 L/min. The high voltage applied to the classifier electrodes was supplied by a DC High Voltage Power Supply (Spellman & Bertran model 602C-10P), with a sweep range of 0.5-2.5 kV.

At a specific applied voltage, the particles exiting the examined classifier constitute an almost singly charged, monodisperse aerosol flow. We then introduced this classified monodisperse flow into a Scanning Mobility Particle Sizer (SMPS) system to measure particle size distribution. The SMPS configuration included a second aerosol neutralizer, a standard Electrostatic Classifier (TSI Model 3082) equipped with a long Differential Mobility Analyzer (DMA) (TSI Model 3081, operated at a 3.0 L/min sheath airflow), and an Ultrafine Condensation Particle Counter (UCPC) (TSI Model 3788). This downstream SMPS system enabled accurate measurement of the particle size distribution, with a mobility-diameter selection range spanning 10 to 700 nm.

The performance evaluation of the miniature electrostatic size classifier is based on several key operational parameters and aerosol characteristics.

Input Challenge Aerosol Metrics: The classifier was tested using polydisperse Sodium Chloride (NaCl) particles generated from a 0.1% NaCl solution. Before entering the classifier, these particles were dried to below 30% relative humidity and neutralized to their Boltzmann charge equilibrium state to prevent electrostatic deposition losses. The resulting challenge aerosol followed a log-normal distribution with the following specific metrics:

1) Mean particle diameter: 98.8 nm

2) Total number concentration: 1.74 x 10^3 particles/cm^3

3) Geometric standard deviation: 2.0

Classifier Operating Parameters: To evaluate its classification capabilities, the device was operated under precisely controlled flow and voltage metrics:

1) Aerosol flow rate (): 0.6 L/min

2) Sheath flow rate (): 1.8 L/min

3) Applied electrode voltage: Swept across a range of 0.5 to 2.5 kV using a DC high-voltage power supply.

Output and Measurement Metrics: The primary performance outcome is the classifier's ability to produce an almost singly-charged, monodisperse aerosol flow at a specific applied voltage. We measured the accuracy of this size classification using a downstream Scanning Mobility Particle Sizer (SMPS) system. This system tracked the output particle size distribution across a mobility-diameter range of 10-700 nm.

Particle normalization is performed using a soft X-ray aerosol neutralizer to stabilize charge. The concentration efficiency is then evaluated across the 10-700 nm range using a UCPC integrated with an SMPS system.

The system's repeatability is determined by the consistency of the monodisperse aerosol output and the stability of the particle size distribution across multiple measurements at the same applied voltage.

D. Mitigation of Particle Loss and Diffusion

The experiments used instruments to manipulate factors affecting particle movement and dispersion, as follows:

1) To ensure stable distribution, wet NaCl particles are processed through a diffusion dryer to maintain relative humidity below 30%RH.

2) A Soft X-ray Aerosol Neutralizer is utilized to reach a Boltzmann charge equilibrium state.

3) This neutralization step is critical to prevent significant particle losses caused by electrostatic deposition on the internal surfaces of the system.

Table II presents an uncertainty budget: voltage ±%, flow rate ±%, dimensional tolerance ±mm, and the expected impact on the classified diameter.

TABLE II
UNCERTAINTY BUDGET TABLE AND IMPACT ON PARTICLE CLASSIFICATION

Source of Uncertainty	Estimated Uncertainty	Expected Impact on Classified Particle Diameter (d_p)
Applied Voltage	±1% to ±2%	**Moderate:** Directly affects electrical mobility. If the voltage is unstable, it shifts the selected d_p, leading to sizing inaccuracies.
Flow Rates	±3% to ±5%	**High:** The ratio of sheath flow (1.8 L/min) to aerosol flow (0.6 L/min) determines resolution. Flow fluctuations cause "peak broadening" in the size distribution.
Physical Dimensions	±0.05 to ±0.1 mm	**Constant:** Uncertainties in electrode spacing or classifier geometry create a systematic bias, causing the actual d_p to deviate from theoretical values.

III. RESULTS AND DISCUSSION

Calculation Setup and Governing Parameters: The particle trajectories within the classifier cavity, situated between the two parallel electrodes, were calculated across a range of operating conditions: Particle sizes from 50 to 200 nm, electrode voltages from 0.5 to 2.5 kV, and total flow rates from 1.8 to 3.0 L/min, all at a constant operating pressure of 1 bar. The calculated results predicted the precise locations where the charged particles were deflected radially and subsequently collected at the electrode surface. Influence of Particle Size (Fig. 5).

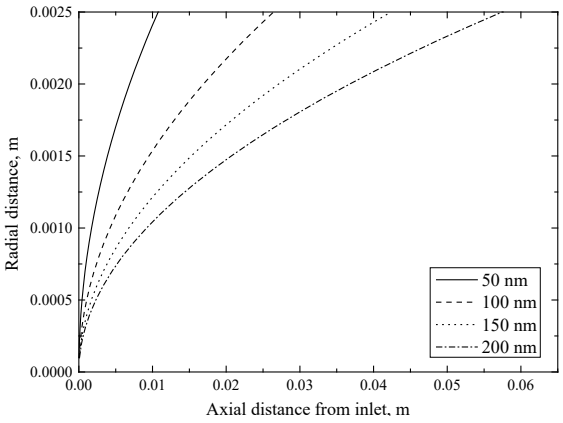

Fig.5. Variation of particle trajectories along the classifier with particle sizes (1.0 kV electrode voltage, 0.6 l/min aerosol flow and 1.2 l/min sheath air flow)

Fig. 5 illustrates how particle size influences the trajectory along the classifier under fixed operating parameters: 1.0 kV inner electrode voltage, 0.6 L/min aerosol flow, and 1.2 L/min sheath air flow. The results clearly indicate that, at a given electrode voltage, smaller particles are collected closer to the classifier entrance slit. This behavior is consistent with their higher electrical mobility, which enables faster migration toward the electrode. Influence of Electrode Voltage (Fig. 6).

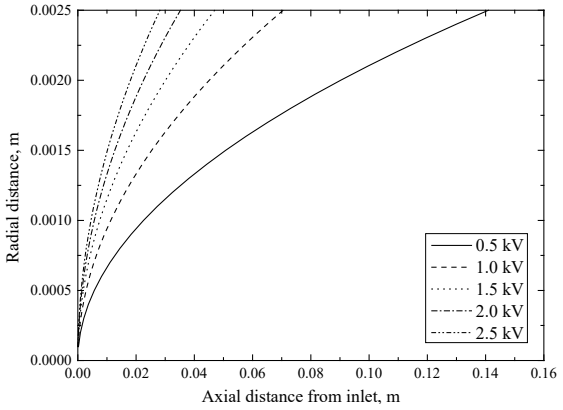

Fig. 6. Variation of particle trajectories along the classifier with electrode voltage (100 nm particle diameter, 0.6 l/min aerosol flow, and 1.2 l/min sheath air flow)

Fig. 6 shows how particle trajectories vary with electrode voltage (100-nm particle diameter, 0.6 l/min aerosol flow, and 1.2 l/min sheath air flow). Increasing the electrode voltage causes a particle of a given size to deposit closer to the entrance slit. This behavior is expected because the applied electrical force primarily determines radial particle motion. A higher voltage intensifies the electric field, increasing the particle's radial velocity. Limitation by Breakdown Voltage: The breakdown voltage imposes an upper limit on the maximum applied electrode voltage.

Given that the breakdown voltage of air is approximately 30 kV/cm under standard conditions (20 °C and 1 bar). Therefore, a 2.5 mm gap between parallel electrodes corresponds to a theoretical breakdown voltage of about 7.5 kV. By applying a significant safety margin to prevent electrical discharge, the electrode system can operate reliably over the 3-5 kV range. Range. Influence of Total Flow Rate (Fig. 7).

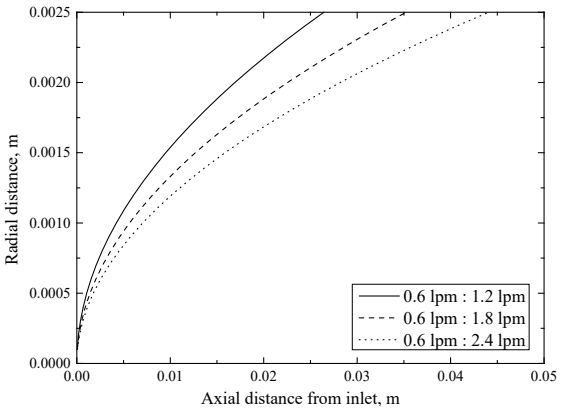

Fig.7. Variation of particle trajectories along the classifier with total flow rate (1.0 kV electrode voltage and 100 nm particle diameter)

Fig. 7 illustrates the variation in particle trajectories as a function of the total flow rate (electrode voltage: 1.0 kV, particle diameter: 100 nm). At higher flow rates, particles of a given size tend to contact the electrode wall further downstream, closer to the exit. This behavior arises because the increased axial flow velocity shortens the particle's residence time within the classification zone, thereby requiring a longer distance to achieve the necessary radial migration. Importantly, the results show that the collection positions for different particle sizes are clearly separated, confirming the classifier's effectiveness. Relationship between Voltage, Flow Rate, and Particle Diameter (Fig. 8).

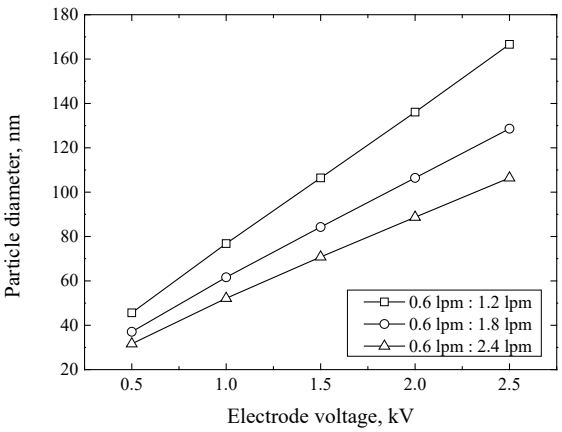

Fig. 8. Variation of the electrode voltage with particle diameter at the aerosol exit slit of the studied classifier at different flow rates

Fig. 8 shows the theoretical and experimental dependence of classified particle diameter on electrode voltage at total flow rates from 1.8 to 3.0 L/min.

The results show two key relationships, consistent with the principles of electrical mobility:

1) Effect of Voltage: Increasing the applied electrode voltage systematically increases the classified particle diameter at the classifier's aerosol exit slit. A higher voltage creates a stronger electric field, enabling larger (lower mobility) particles to migrate toward the collection electrode within the classification zone.

2) Effect of Flow Rate: Conversely, increasing the total flow rate results in a decrease in the classified particle diameter for a constant voltage. A higher flow rate reduces the residence time of the particles within the classification zone, meaning only smaller (higher mobility) particles can complete the necessary migration distance before exiting.

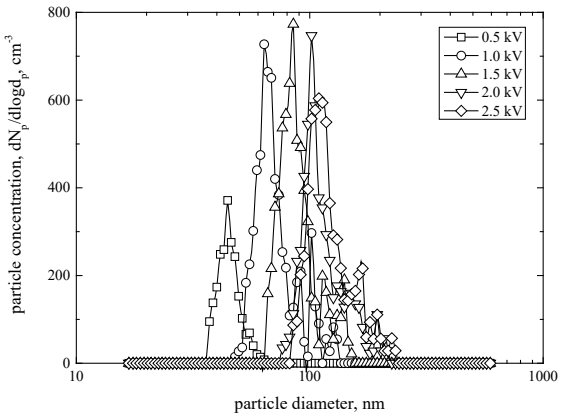

Fig. 9. Particle size distribution of the studied miniature electrostatic classifier at different electrode voltages

This behavior confirms that the classified particle size depends on electrode voltage, total flow rate, and the particle's electrical mobility. Since smaller particles have higher electrical mobility than larger ones, the classifier can precisely select the desired size by controlling the applied voltage and flow parameters. Monodisperse Particle Generation (Fig. 9)

Fig. 9 presents the size distribution of particles exiting the classifier, obtained by sweeping the applied electrode voltage from 0.5 to 2.5 kV. Throughout this experiment, the total operating flow rate was maintained at approximately 1.8 L/min.

The results clearly demonstrate that the particles exiting the classifier at any given voltage are highly monodisperse. This validates the effectiveness of the developed miniature electrostatic classifier for precise particle-size selection. As shown in Fig. 10, the particle-size distribution of the monodisperse aerosol exiting the classifier was evaluated at various applied electrode voltages. Classification Performance: The experimental results confirm that the miniature electrostatic classifier produced an approximately monodisperse size distribution at the aerosol exit slit.

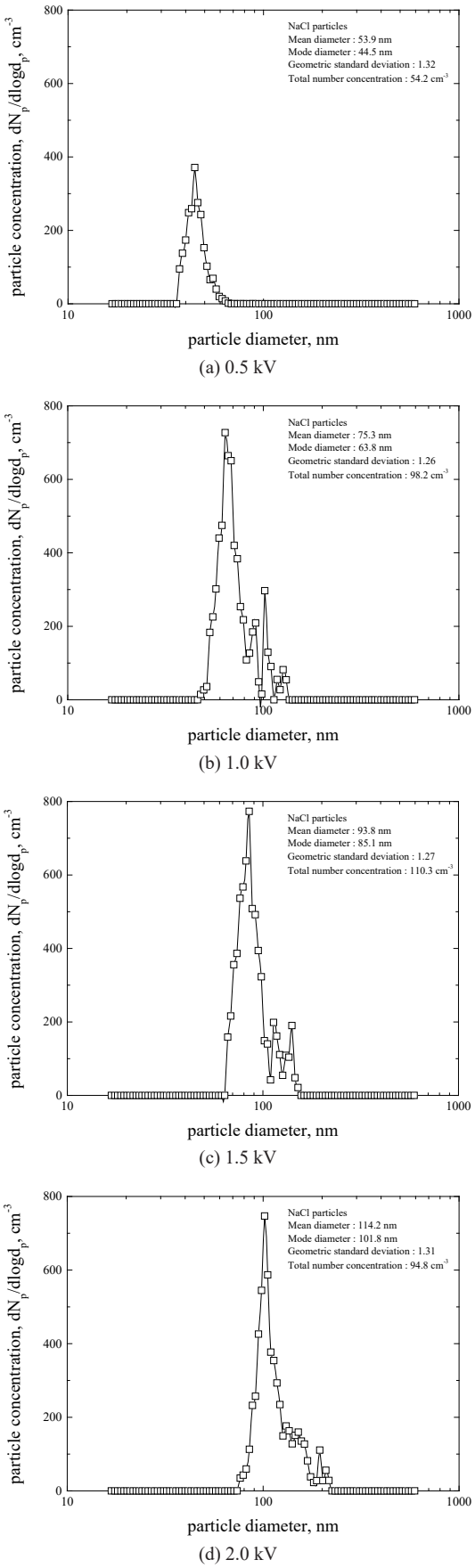

Fig. 10. Particle size distribution of monodisperse aerosol at different electrode voltages

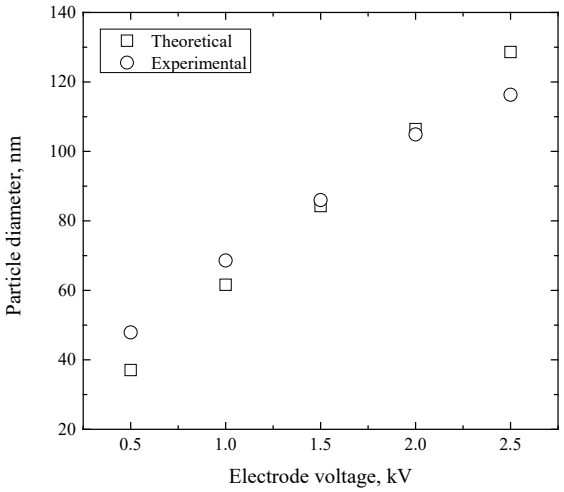

Fig. 11. Theoretical and experimental variation of the electrode voltage with particle diameter (0.6 l/min aerosol flow and 1.2 l/min sheath air flow

For applied electrode voltages of 0.5, 1.0, 1.5, 2.0, and 2.5 kV, the corresponding mean particle diameters ($D_{p,\text{mean}}$) were approximately 53.9, 75.3, 93.8, 114.2, and 126.7 nm, respectively. The geometric standard deviations (sigma_g) calculated for these classified mean diameters were 1.32, 1.26, 1.27, 1.31, and 1.28, respectively. These low sigma_g values clearly indicate the classifier's high efficiency at generating a narrow, monodisperse output. Observation of Multiply-Charged Particles

Multiply-charged particles began to appear in the classified aerosol distribution when classifying particles larger than 100 nm. This phenomenon is typical of electrical mobility classifiers and is a critical factor when interpreting size-classification data in this range.

Fig. 11 illustrates the theoretical and experimental relationship between the applied electrode voltage (kV) and the resulting classified particle diameter (nm) under fixed operating conditions: 0.6 L/min aerosol flow and 1.2 L/min sheath air flow. Key Findings and Discussion

1) Agreement in Trend: The overall trend observed in the experimental measurements (circles) closely mirrors the tendency predicted by the theoretical model (squares). Both curves show a clear positive correlation: as the electrode voltage increases, the classified particle diameter increases, consistent with the fundamental principles of electrical mobility classification.

2) Magnitude Discrepancy: While the trends align, a systematic deviation is observed between the two datasets. The discrepancy is smallest at 2.0 kV but becomes more pronounced at both lower and higher voltages. In general, the experimental particle diameters are consistently lower than the theoretically predicted diameters for the same voltage.

3) Potential Cause of Discrepancy: This disparity between the experimentally measured mean particle diameter and the theoretical prediction is primarily attributed to the influence of multiply-charged particles entering the classification zone. Multiply charged particles (e.g., a 2q particle) would be measured to have an electrical mobility diameter smaller than their true size at a given voltage, thus shifting the experimental data downward. Further investigation is warranted to fully explore and quantify the underlying causes for this discrepancy in both the theoretical assumptions and experimental conditions.

V. Conclusion

In summary, your argument is very valid. This article shows that experimental trends strongly agree with theoretical models for sizes up to 126.7 nm at 2.5 kV. However, the device has not yet been empirically proven to operate at the 300 nm level, consistent with the design's potential. To demonstrate its capability in the 300 nm range, further research is needed, as the author suggests, including modifications to the experimental methods, such as using larger starting aerosols or employing techniques to remove multi-charge fractions before measurements.

Experimental evaluation of the prototype using NaCl particles (0.6 L/min aerosol flow, 1.8 L/min sheath flow) and an applied voltage ranging from 0.5 to 2.5 kV demonstrated initial nanoparticle classification capabilities. However, SMPS measurements showed a significant magnitude discrepancy relative to theoretical predictions, indicating that the current mathematical model does not fully account for real-world particle behavior. Further refinement of both the physical design and theoretical framework is required to enhance classification accuracy.

Table III and Fig. 12 summarize the data, demonstrating that as the voltage rises from 0.5 kV to 2.5 kV, the measurement error drops substantially from 45.7% down to 1.0%.

TABLE III
PROVIDE A SUMMARY TABLE: VOLTAGE, PREDICTED DP, MEASURED DP (MEAN/MODE), SIGMA_G, ERROR (%)

Voltage (kV)	Mean d_p (nm)	Mode d_p (nm)	GSD (σ_g)	Predicted d_p (nm)	Error (%)
0.5	53.9	44.5	1.32	37	45.7
1.0	75.3	63.8	1.26	62	21.5
1.5	93.8	85.1	1.27	84	11.7
2.0	114.2	101.8	1.31	107	6.7
2.5	126.7	113.2	1.28	128	1.0

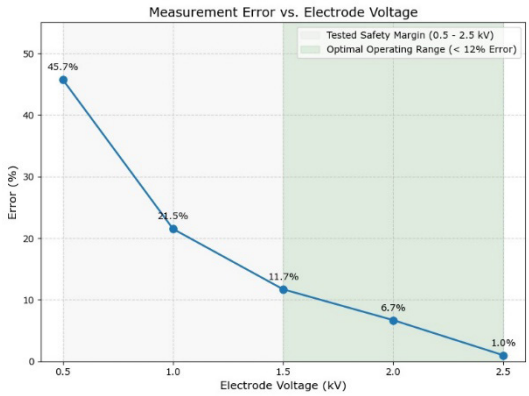

Fig. 12. Effect of Electrode Voltage on Measurement Error

VI. Recommendations for Future Research

Based on this work, the following specific directions are recommended for future research, covering both theoretical and experimental aspects of electrical mobility analyzer development:

1) Expand Detection Range and Multi-Parameter Sensing: Future work should focus on expanding the measurable size range to allow a single sensor to cover a broader spectrum of naturally occurring particles. Furthermore, integrating the mESC with other measurement techniques would enable multi-parameter investigations, facilitating the simultaneous quantification of nanoparticles (from molecular clusters up to 100 nm) and analysis of characteristics beyond size, such as composition.

2) Design Optimization and Manufacturing Precision: Further investigation is essential to refine the analyzer's design. This research should quantify the impact of several critical factors on classification performance and accuracy, including design configuration; limitations imposed by manufacturing precision and practical materials; non-ideal flow conditions; electrode eccentricity; component misalignment; and the accuracy of flow-setting mechanisms.

3) Non-Spherical Particle Analysis: The performance and accuracy of the analyzer must be evaluated when classifying non-spherical aerosol particles, such as asbestos fibers, soot aggregates, or bio-aerosols, commonly found in nature. Because particle shape strongly influences drag, settling velocity, and electrical mobility (non-spherical particles generally have lower electrical mobility than spherical particles), understanding this effect is crucial for real-world applications.

4) Enhanced Temporal Response: To accurately assess the transient behavior of airborne particles, such as those found in automotive exhaust gas, the temporal responsiveness (response time) of the instrument should be significantly improved.

Acknowledgements

The authors gratefully acknowledge the financial support provided by the Thailand Center of Excellence for Life Sciences (TCELS) under Research Contract No. TC-A (ERP) 15/2564.

References

[1] P. R. Sune et al., "Nanoparticles: Classification, types and applications: A comprehensive review," *GSC Biol. Pharm. Sci.*, vol. 29, pp. 190-197, Dec. 2024.

[2] Z. Sung et al., "Direct observation of nanometer size hydride precipitations in superconducting niobium," *J. Springer,* vol.14, pp. 1-12, Nov. 2024, https://doi.org/10.1038/s41598-024-77905-6

[3] S. M. Tham and M. Daley, "Measurement of gas concentrations," *J. Sci.*, vol. 25, p.128-132, Feb. 2024.

[4] I. Ueta, "Gas chromatographic determination of volatile compounds," *J. Springer,* vol. 38, pp. 737-738, Apr. 2022, https://doi.org/10.1007/s44211-022-00108-4

[5] X. Kong, M. Ammann, C. George, and D. Knopf, "Atomic and molecular ions in atmospheric chemistry: Interfacial reactivity, emerging mechanisms, and future perspectives," *J. Geophys. Res.: Atmos.*, vol. 130, no. 20, Art. no. e2025JD044379, Oct. 2025, https://doi.org/10.1029/2025JD044379

[6] Y. Li, W. Yang, H. Lin, and Z. Kuang, "Research on suspended particle size measurement based on ultrasonic backscattered amplitude analysis," *J.* MDPI, vol. 16, pp. 2-13, Jun. 2024, https://doi.org/10.3390/w16141973

[7] R. C. Flagan, "History of electrical aerosol measurements," *Aerosol Sci. Technol.*, vol. 28, no. 4, pp. 301-380, Apr. 1998, https://doi.org/10.1080/02786829808965530

[8] P. Intra and N. Tippayawong, "An overview of differential mobility analyzers for size classification of nanometer-sized aerosol particles," *J. Science and Technology*, vol. 30, no. 2, pp. 243-256, Mar. 2008.

[9] K. T. Whitby and W. E. Clark, "Electric aerosol particle counting and size distribution measuring system for the 0.015 to 1 μ size range," *Tellus*, vol. 18, no. 2-3, pp. 573-586, Aug. 1966, https://doi.org/10.3402/tellusa.v18i2-3.9340

[10] K. Vasilatou et al., "Aerosol physical characterization: A review on the current state of aerosol documentary standards and calibration strategies," *J. Aerosol Sci.*, vol. 183, Art. no. 106483, Jan. 2025, https://www.sciencedirect.com/science/article/pii/S0021850224001502

[11] A. Barba-Lobo, E. G. San Miguel, and J. P. Bolívar, "A new procedure to validate and optimize ^210Po measurements in atmospheric aerosols," *J. Aerosol Sci*., vol. 183, Art. no. 106469, Jan. 2025, https://www.sciencedirect.com/science/article/pii/S0021850224001368

[12] S. Basnet, A. Jäntti, P. Yli-Pirilä, M. Kortelainen, O. Sippula, and A. Lähde, "Performance of dry electrostatic precipitator for the removal of CsI aerosol particles under simulated severe nuclear accident conditions," *Nucl. Eng. Des*., vol. 445, Art. no. 114440, Dec. 2025, https://www.sciencedirect.com/science/article/pii/S002954932500617X

[13] J. Wu et al., "Effect of filter rod structure on aerosol particle size distribution in electrically heated cigarettes," *Atmos. Environ.: X*, vol. 29, Art. no. 100412, Jan. 2026, https://doi.org/10.1016/j.aeaoa.2025.100412

[14] H. Hagino, "Winter emission factors of ultrafine total and solid particle numbers and PM2.5 near a major arterial road in Tokyo," *Atmos. Environ.: X*, vol. 28, Art. no. 100382, Dec. 2025, https://doi.org/10.1016/j.aeaoa.2025.100382

[15] A. Bianco et al., "Separation of isomers using a Differential Mobility Analyser (DMA): Comparison of experimental vs modelled ion mobility," *Talanta*, vol. 243, Art. no. 123339, Jun. 2022, https://doi.org/10.1016/j.talanta.2022.123339

[16] C. Hagwood, Y. Sivathanu, and G. Mulholland, "The DMA transfer function with Brownian motion: A trajectory/ Monte-Carlo approach," *Aerosol Sci. Technol.*, vol. 30, no. 1, pp. 40-61, Jan. 1999, https://www.tandfonline.com/doi/abs/10.1080/027868299304877

[17] M. Carsí and M. Alonso, "A simple correlation to estimate the resolution of concentric cylindrical DMAs for diffusive particles," *J. Aerosol Sci.*, vol. 167, Art. no. 106089, Jan. 2023, https://doi.org/10.1016/j.jaerosci.2022.106089



Papol Sardyoung is currently an Assistant Professor in the Department of Industrial Electrical Technology, Faculty of Industrial Technology, Thepsatri Rajabhat University, Lopburi, Thailand.

He researches pulsed electric fields, Energy Conversion, energy-saving for Industry, and solar cell design and Simulation.



Panich Intra is currently an Associate Professor working at the Electro-Aerosol Instrument Laboratory (EAIL), Research Unit of Applied Electric Field in Engineering (RUEE), the College of Integrated Science and Technology, Rajamangala University of Technology Lanna, Chiang Mai, Thailand.

He researches aerosol electrical mobility analysis, Corona discharge-based aerosol charging, Electrostatic precipitation, and Pulsed electric field and electroporation. Current projects include "Modification, calibration, and field testing of an electrical particulate matter monitor towards commercialization" and "Development of a microorganism inactivation system in beverage production processes for industrial use using a pulsed electric field technique."